

AIAS 2018 International Conference on Stress Analysis

## 3D strip model for continuous roll-forming process simulation

Luca Esposito<sup>a\*</sup>, Alcide Bertocco<sup>a</sup>, Raffaele Sepe<sup>a</sup>, Enrico Armentani<sup>a</sup>

<sup>a</sup>University of Naples Federico II, P.le V. Tecchio 80, 80125 Naples, Italy

---

### Abstract

The paper addresses the complexities for a reliable numerical simulation of the roll forming process. During the process, the material is progressively bent accumulating plastic deformation at each forming step. Strain hardening limits the material formability and may causes flaws of the final shape. A simplified method for the FEM modeling of the process has been developed introducing a narrow-strip 3D model. This approach leads better performance than the classical modeling method, in terms of results reliability and low computational time. In order to verify the proposed model, an experimental campaign of testing, for a specific roll forming production process, was carried out. On the quasi-static regime, the post necking behavior of the sheet metal was characterized. The Vickers hardness and the plastic strain of uniaxial tests were empirically correlated. By the hardness correlation, the plastic strain accumulated at different stages of the process was evaluated and compared with the numerical results. Further possible improvements of the method are highlighted.

© 2018 The Authors. Published by Elsevier B.V.

This is an open access article under the CC BY-NC-ND license (<http://creativecommons.org/licenses/by-nc-nd/3.0/>)

Peer-review under responsibility of the Scientific Committee of AIAS 2018 International Conference on Stress Analysis.

*Keywords:* Roll forming, FEM analysis, Strain-Hardness correlation

---

\* Corresponding author. Tel.: +39-0817682463;  
*E-mail address:* [luca.esposito2@unina.it](mailto:luca.esposito2@unina.it)

### 1. Introduction

Cold roll forming is a continuous deformation process to produce long shapes of essentially uniform cross-section starting from strip or coiled metal sheet. Generally, cold formed parts are forged in a number of stages and in each one the material is fed through multiple pairs of contoured forming rolls, which progressively shape the metal until the desired cross section is produced. To increase the machine durability oil-hardened tool steel is commonly used for

the rolls. Roll forming is typically a high volume production process. Theoretically, unlimited length can be shaped as the material need only pass through the roller dies. The manufacturing process finds wide application in automotive, building, construction, office furniture and aircraft industries. Both ferrous and non-ferrous metals as well as some non-metallic material can be roll formed. Mild steel and aluminum are the most common materials used in the process. Additionally, polished, painted, coated and plated materials can also be roll formed. The process complexity depends by the desired profile as well as by the mechanical properties of the material to be formed. The material undergoes additional permanent deformation at each forming stage. The roll forming is a progressive process therefore the number of forming passes is generally optimized. Too few passes can cause excessive deformations, distortion and loss of tolerance; too many passes increase the final cost for production. Nowadays CAD software packages are very useful in roller design, however to prevent production defects, the material behaviour under large deformation must be taken into consideration, Wang et al. (2016). In this perspective, the finite element method (FEM) analysis of the entire process can be a useful tool for the roll forming machine optimization, Wang et al. (2018). Main advantage of numerical simulations in this field is the better understanding of the material behaviour during deformation accounting for the effect of production parameters variation such as rolls shape, forming material and metal sheet thickness. On the other hand, this type of simulation is very complex and often expensive in terms of computational time. Numerical issues are related to: a) multiple contact bodies and self-contact; b) large displacements; c) large plastic deformations; e) friction; d) triaxiality of the state of stress. The validation of the roll forming simulations is another open issue that needs to be examined.

## 2. Method

The present study checked the virtual reproducibility of the manufacturing process by two numerical approaches; the first one is a classical dynamic explicit analysis using LS-Dyna and the second uses the implicit solver of the MSC/Marc with a simplified 3d strip model. A real roll forming process was considered and its most critical steps were simulated by finite element methods. Galvanized structural coil of S320GD steel grades is the rolled material. The starting flat product is a metal sheet with thickness of 1.5mm. The chemical composition of the material is given in table 1. The anisotropic behaviour of the material was investigated by testing uniaxial samples with loading axis at 90°, 45° and 0° degrees respect to the rolling direction. During the process the material progressively bent at each stand, accumulating plastic deformation mainly in the 90° direction. For that reason, the sheet was simulated as isotropic material with the elasto-plastic properties obtained from tests of flat specimens cut orthogonally to the rolling way. Since during profiling large deformation is expected, the flow stress curve of the metal sheet was entirely identified up to the failure. For the identification of the post necking behaviour an inverse calibration procedure using FEM simulation of the tensile test was adopted. Various uniaxial tests at different values of strain, measured by extensometer, were carried out and then their Vickers hardness was measured too. In this way, it was possible to find a correlation between plastic strain and hardness; about that an exponential law was proposed. Samples of material were extracted at different steps of the working process and Vickers hardness measurements were performed. That values by means of the aforementioned law allow to estimate the evolution of the maximum local strain. The maximum strain prediction is greatly important since the plastic strain is the principal parameter causing the ductile damage of metals and it is commonly considered into several failure criteria (Lemaitre (1985); Bonora (1997); Bonora et al. (2006); Lombardi et al. (2009)). To validate the modeling, the plastic strain accumulated at different stages of the process was evaluated and compared with the numerical results.

Table 1. Chemical composition of S320GD (max. %)

Steel Grade	Coating symbol	C	Si	Mn	P	S
S320GD	+Z	0.20	0.60	1.70	0.10	0.045

### 3. Profile description and flower design

The analyzed roll forming process produces a classical window frame's profile of cross section 60x40 millimeters whose nominal dimensions are shown in figure 1a. In particular, the 180° fold of the cross section, highlighted in figure 1b, was taken as case study for the simulations. The fold requires 13 steps of deformation induced by 26 pairs of contoured forming rolls and 4 lateral forming rolls. Flower pattern of the rolling process is the station-by-station overlay of the progressive part contours starting with the flat strip width before forming and ending with the final desired section profile. In the present study, the flower design involves 13 steps with a bend angle that increases by 15 degrees at each step. The maximum production velocity is 40 meters per minute as result of the rolls dragging.

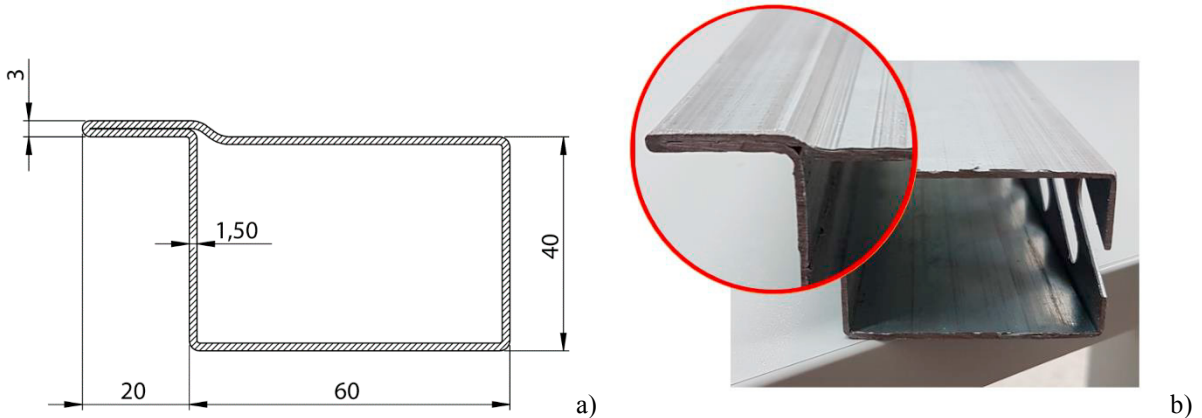


Fig. 1. a) Nominal dimensions of the cross section profile; b) Picture of the produced profile with the 180° fold highlighted.

### 4. Material characterization

The standard uniaxial tensile test on thin sheet specimens with a rectangular cross-section is the most popular method for acquiring the flow curve of sheet metal materials, Tvergaard (1993). Standard uniaxial tests with loading axis at 90°, 45° and 0° degrees respect to the rolling direction of the metal sheet were conducted. The experimental engineering stress-strain curves are compared in figure 2. The material along the different directions performs very similarly. However, the 90° curve was considered as the most representative for the roll forming process and it was further processed to get the true stress-strain curve up to failure. As suggested by Lange (1985), the influence of the strain rate on the flow stress is usually small during cold forming processes, thus in this study it has been neglected. The equally strained portion of the tested uniaxial samples, independently from the cutting directions, are used for micro-Vickers hardness tests.

#### 4.1. Post necking characterization

The true stress-strain curve can be achieved up to the maximum uniform elongation point using conventional measurement techniques such as strain gauges or extensometers. Once diffuse necking occurs, the stress and strain distributions over the necking area become heterogeneous, Kim et al. (2013). In the present study, the engineering strain up to 20% was measured by 25mm extensometer on the specimen gauge length. The flow stress curve beyond the necking point was determined by inverse method based on FE model updating. According to the Considère criterion, the necking initiates when the value of true stress ( $\sigma_t$ ) reaches the strain-hardening rate ( $\partial\sigma_t/\partial\varepsilon_t$ ), Yang et al. (2017). Using this criterion the necking was recognized at about 11% of true strain. The post necking behaviour was identified as follow: the estimated true stress-strain curve is fed into the FE program and the simulated result is compared with the experimentally measured data. The measurements needed for comparison purposes is the load-axial displacement curve. A minimization of the discrepancy between the computed and experimental data is carried

out iteratively changing the post necking flow stress curve. The output of the optimization procedure in terms of true stress-strain and load-displacement curves is reported in figure 3.

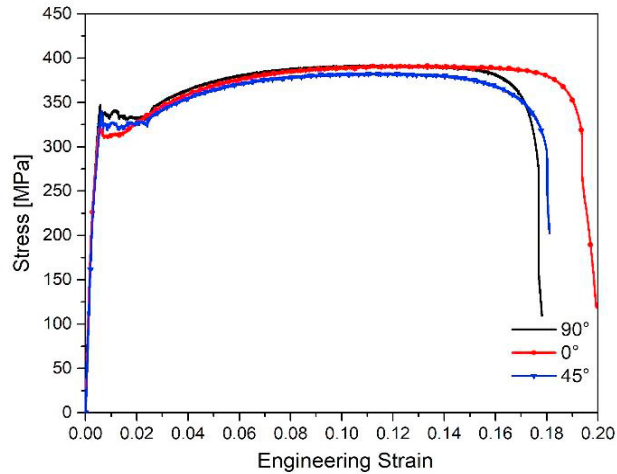


Fig. 2. Effect of loading orientation on engineering stress-strain curves.

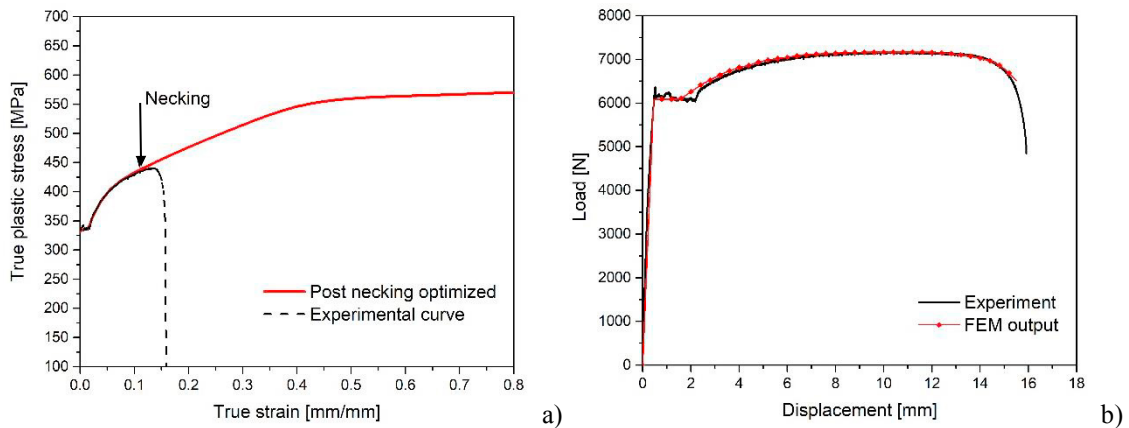


Fig. 3. Output of the optimization procedure in terms of true stress-strain (a) and load-displacement curves (b).

#### 4.2. Strain - Hardness correlation

The accumulated strain during the process is the fundamental variable driving the damage mechanism of the metal sheet. The capability of the numerical analysis to predict the plastic strain accumulation was checked. The local evolution of the strain during the roll forming was inversely evaluated by hardness measurements. In literature several correlation between plastic deformation and hardness are proposed, Sonmez and Demir (2007). In the present work, the following phenomenological correlation between the hardness ( $Hv$ ) and the plastic strain ( $\varepsilon_p$ ) is proposed:

$$Hv = Hv_0 + K \varepsilon_p^n \quad (1)$$

where  $Hv_0$  is the nominal hardness of the metal sheet and  $K$  and  $n$  are material constants. The parameters of Eq. 1 were identified by non-linear regression fitting using hardness measurements performed on tensile tested specimens

that had achieved a fixed value of deformation. Micro-Vickers hardness tests were conducted according to the standard EN ISO 6507 (2018). The best fitting curve and the identified parameters are shown in figure 4. Portions of the metal sheet were extracted at six different stages of the rolling process and then were prepared to evaluate the hardness near the selected fold. After the waterjet cutting, samples encapsulation and polishing was carefully executed to preserve physical characteristics of the metal. Samples prepared for micro-Vickers test are shown in figure 5. Five hardness measures for each samples along the bending extrados were performed. The process plastic strain was evaluated inferring the hardness in Eq. 1 which values are summarized in table 2 together with the fold angle. The hardness mean value with standard deviation as function of the true plastic strain is plotted in figure 6.

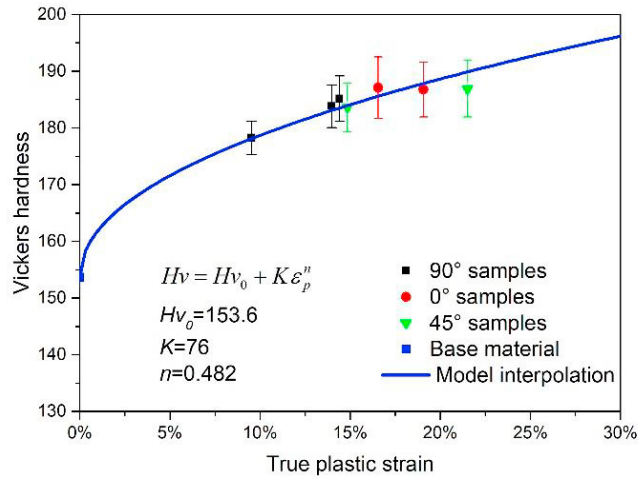


Fig. 4. Best fitting for strain-hardening correlation.



Fig. 5. a) Samples for micro-Vickers.

Table 2. Plastic strain evaluation by Micro-Vickers measurements at different rolling stages

Rolling stage	Fold angle	HV (mean)	Plastic strain
3	30°	153.66	9%
6	75°	177.05	36%
9	120°	200.80	61%
12	165°	213.35	82%
13	180°	222.67	79%

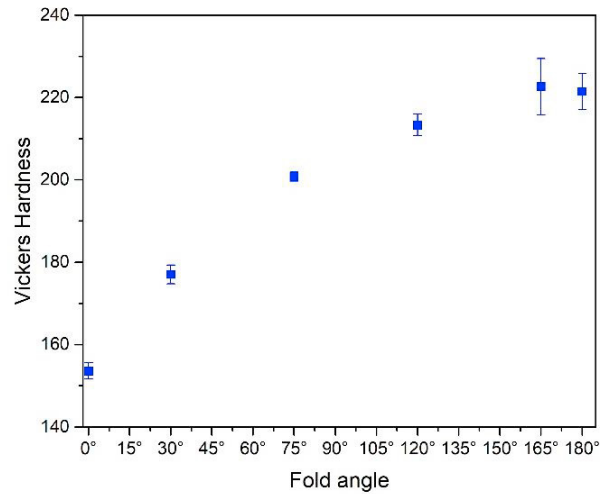


Fig. 6. Measurements of micro-Vickers hardness as function of the fold angle

## 5. FE models

Due to the complexity of the process, the following simplifications of the problem for both the simulations are assumed: 1) no friction is considered; 2) rolls are modelled as rigid bodies; 3) isotropic hardening for the metal sheet is assumed; 4) zinc coating effect is neglected. The metal sheet is considered fixed in rolling direction while the rolls are moved toward the part. The rotation of rolls needed for the physical dragging of the metal sheet, was proved to have negligible effect on simulations, thus for a better convergence it was not implemented. Further computational features specific for each approach are detailed below.

### 5.1. Explicit analysis

The extensive process simulation was performed by the finite element code Ls-Dyna® in explicit time integration. The simulated metal sheet is 300 mm long, enough to reproduce contemporary contact at contiguous deformation stages. The metal sheet mesh counts 5600 shell elements using the Belytschko-Tsay formulation, with five integration points through the thickness. The minimum longitudinal dimension of the element is 1.56mm. The Lobatto rule for integration points positioning was used to allow the extraction of element variables near the location of interest. Further details on the Belytschko-Tsay formulation and the Lobatto rule can be found in LS-DYNA (1998). Automatic single surface is the contact algorithm implemented. In figure 7, the complete layout of the model at the beginning of the analysis is shown. In order to stabilize the analysis and reduce the sliding interface energy, the scale factor for computed time step is adequately reduced. Furthermore, in order to improve results accuracy, it is set that membrane straining can causes thickness change. This option is important for sheet metal forming or whenever membrane stretching is significant.

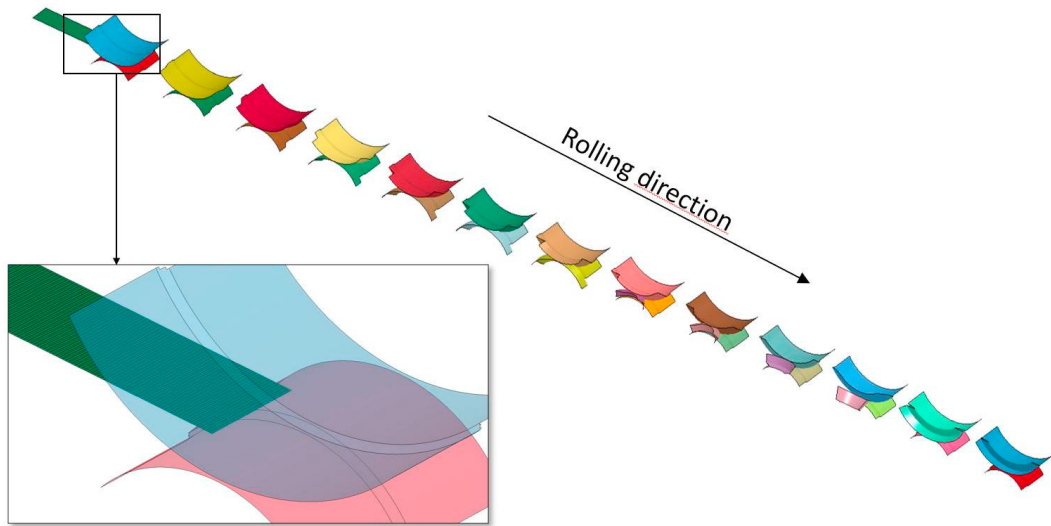


Fig. 7. Arrangement of rolls and detail of the mesh for the dynamic analysis

### 5.2. Implicit 3D strip modeling

Aim of the proposed 3D strip model is to preserve most of numerical information of a reliable simulation with a reduced computational time. Since the process simulation requires many fine-tunings, the computational time becomes a crucial aspect of the analysis. A narrow strip of 6mm in the rolling direction and 94mm orthogonally to the rolling direction was meshed. The dimension of the strip in rolling direction is quite small to avoid contemporary contact at contiguous deformation stages. The overlapping of rigid surfaces defining rolls is permitted as rigid-to-rigid contact is not defined. This allows to reduce the distance between roll stands and consequently the total computational time. Nine-node, three-dimensional, first-order isoparametric element was selected. Assumed strain and constant dilatation options were activated to increase the performance of the element during the bending process, further details can be found in MSC.MARC (2014). With the transition to the plastic state the current coefficient of the lateral deformation tends to  $\nu = 0.5$  and the Herrmann formulation gives good stability to the analysis. The Herrmann formulation, generally used for state of incompressibility, uses the ninth integration point at the center to evaluate the pressure assumed constant throughout the element. Updated Lagrange procedure and finite strain plasticity formulation is assumed. In order to consider a refined mesh and reduce the calculation time, the region interested by the folding area was meshed with 4 elements into the thickness while 2 elements were adopted elsewhere. Furthermore, to improve the accuracy of the solution at higher fold angles, the number of elements and nodes was locally increased using the adaptive mesh generation. The local remeshing procedure works by dividing an element introducing the new node on an edge in midside to the two corner nodes, MSC.MARC manual (2014). The adopted criteria causes the subdivision of the elements when overcoming of 40% of plastic deformation occurs.

## 6. Results analysis

The 3D strip model having a better discretization of the folding area, allows a more detailed description of the strain field. It was found that the location of the maximum strain could likely change during the folding process as

effect of the rolls configuration. In order to capture the real maximum strain on the fold, a path of sample points at the extrados of the curvature was selected and the evolution of the equivalent plastic strain along the path at different deformation steps is reported in figure 8a. The sample points used for the strain extraction are shown in figure 8b on the mesh under deformed configuration at the stage 6. The numerical bending progression is visible by the flower assembled in figure 9. The deformed mesh at the end of each stage reflects the rolls geometry and configuration. The numerical maximum value of the true plastic strain at each deformation step is compared with the corresponding value estimated by hardness measurement. Both explicit and 3D strip model are consistent with experimental data. As shown in figure 10, the 3d strip model slightly overestimates the accumulated plastic strain at low fold angle respect to the experiments and the dynamic analysis. Nevertheless, the real strain state produced by the cold rolling process is difficult to evaluate and affected by large variability which probably justifies the difference of few percentile found. In terms of computational time, the 3d strip model is extremely more rapid. Using the same workstation (Intel® Xeon® X5650 processor and 36GB RAM DDR3), about 20 hours instead of 15 minutes is the calculus time required for the dynamic and the 3d strip model analysis respectively.

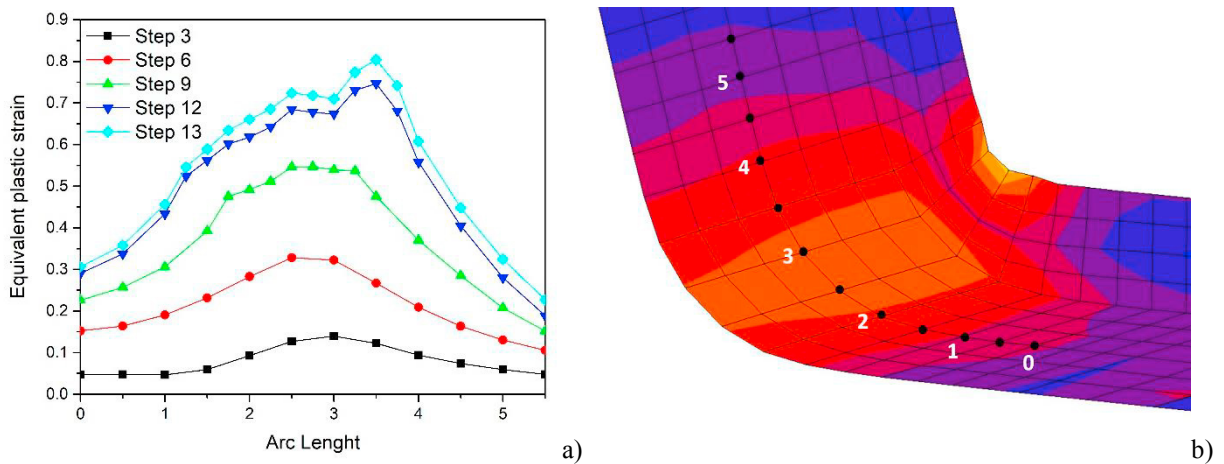


Fig. 8. Evolution of equivalent plastic strain (a) at sample points (b)

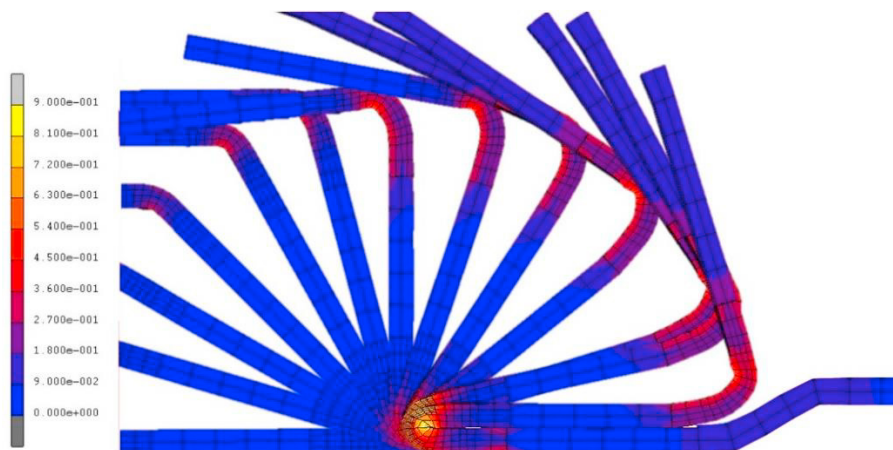


Fig. 9. Flower pattern of the process numerically obtained



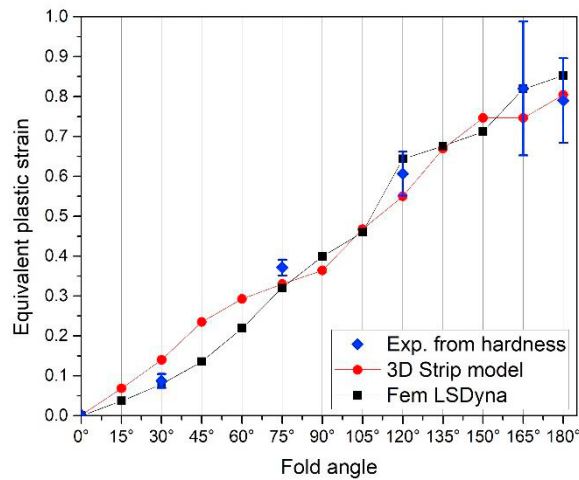


Fig. 10. Comparison of the predicted equivalent true plastic strain and the experimental values as function of the fold angle

## 7. Conclusions

The cold roll forming deformation can be helpfully simulated by finite element modeling. Since the process complexities, some numerical strategies for the simplification of numerical analyses are desirable. A 3D strip implicit model is here proposed as alternative to a widespread metal sheet simulation. A sequential logic of deformation steps is adopted and the metal sheet stretching is neglected. This approach leads to good results in terms of local plastic strain accumulation with the benefit of a very low computational time. Process defects as the bowing are affected by friction, pressure induced by rolls and distance between rolls pair. Evidently, that kind of defects cannot be reproduced or predicted by a narrow strip model but a whole approach simulation is required. However, the 3D strip model could be usefully used to predict ruptures induced by excessive deformation or to highlight the formability limit of new material for preexisting equipment layout. The proposed model allows a better calculation of the strain field and stress triaxiality resulting more suitable for the implementation of damage models.

## Acknowledgements

The authors wish to thank Dr. Salvatore Gambardella and the Tecnosistem s.r.l. for providing of samples and the roll-forming equipment.

## References

- Bonora N., "A nonlinear CDM model for ductile failure" *Engineering Fracture Mechanics*, 58, (1-2), 1997, 11-28.
- Bonora N., Ruggiero A., Esposito L. Gentile D. "CDM modeling of ductile failure in ferritic steels: Assessment of the geometry transferability of model parameters" *International Journal of Plasticity*, 22 (11), 2006, 2015-2047.
- EN ISO 6507 standard "Metallic materials – Vickers hardness test – Part1: Test method", 2018.
- Kim, J.-H. et al. "Characterization of the post-necking strain hardening behavior using the virtual fields method" *International Journal of Solids and Structures*. 50, 2013, 3829-3842.
- Lange K, editor. *Handbook of metal forming*. New York: McGraw-Hill Book Company; 1985.
- Lemaitre J. A. "A Continuous Damage Mechanics Model for Ductile Fracture", *Journal of Engineering Materials and Technology*, 107, 1985, 83-89.
- Lombardi P., Cipolla L., Folgarait P., Bonora N., Esposito L. "New time-independent formulation for creep damage in polycrystalline metals and its specialisation to high alloy steel for high-temperature applications" *Materials Science and Engineering A*, 510-511, issue C, 2009, 214-218.

- LS-DYNA, Livermore Software Technology Corporation, Theoretical Manual, May 1998.
- MSC.MARC, MSC Software Corporation, Volume A: Theory and User Information, 2014.
- Sonmez F. O., Demir A. “Analytical relations between hardness and strain for cold formed parts” *Journal of Materials Processing Technology*, 186, 2007, 163–173.
- Tvergaard, V. “Necking in tensile bars with rectangular cross-section.” *Computer Methods in Applied Mechanics and Engineering*, 103, (1), 1993, 273–290.
- Wang H., Yan Y., Jia F., Han F. “Investigations of fracture on DP980 steel sheet in roll forming process” *Journal of Manufacturing Processes*, 22, 2016, 177-184.
- Wang X.G., Liua X.H., S. Wang, Zhi Y. “Experiment and simulation to rolled profile strip with variable thicknesses in lateral direction” *Journal of Materials Processing Tech.*, 258, 2018, 259-270.
- Yang C.L. et al. “The premature necking of twinning-induced plasticity steels” *Acta Materialia*, 136, 2017, 1-10.